

Propagation of Hydromagnetic Waves in the Magnetosphere¹

Masahisa Sugiura

NASA, Goddard Space Flight Center, Greenbelt, Md.

(Received February 3, 1965; revised April 5, 1965)

Characteristics of waves in a two-component cold plasma are reviewed. Using the Clemmow-Mullaly-Allis diagram, the topological types of the wave-normal surfaces are shown. A consistent system of labeling the modes, initially given by Allis, is explained. Reversal in the polarization in the electric field is examined, and all the modes in which the reversal occurs are specified. There is no polarization reversal in ULF to VLF waves in the magnetosphere. The lower hybrid resonance frequency in the magnetosphere is discussed.

The equations of motion for an electromagnetic ray are derived. Defining the action for the ray with analogy to that for a particle in classical mechanics, the principle of least action is proved. It is shown that if the dispersion relation is homogeneous in the wave vector and the frequency, the principle of least action implies the principle of least time, i.e., Fermat's principle. When the principle of least time holds, as is the case with Alfvén compressional waves, the trajectory of a ray can be determined from a variational equation, from which the problem can be formulated in Hamiltonian form. For the axially symmetric case, the generalized momentum conjugate to the azimuthal coordinate is a constant of motion. Using this relation, "allowed" and "forbidden" regions are defined when a set of initial conditions for the ray is given. This method is applied to a model magnetosphere with a dipole magnetic field. It is shown that the accessibility of hydromagnetic rays originating from the boundary of the magnetosphere to the earth is greatly limited. For a distorted magnetosphere the canonical equations for a hydromagnetic ray are integrated by a numerical method. Typical trajectories in the equatorial plane are shown, and the effects of the deformation of the dipole field on the ray trajectories are discussed.

1. Introduction

Propagation characteristics of hydromagnetic waves can be seen in a proper perspective relative to other modes of electromagnetic waves by reviewing plasma waves in general without imposing restrictions on wave frequency or on plasma parameters. This approach is taken in the present paper, and for the representation of modes we use the Clemmow-Mullaly-Allis diagram (abbreviated as the CMA diagram below) of wave-normal surfaces [for details of the CMA diagram see Clemmow and Mullaly, 1955; Allis, 1959; Allis, Buchsbaum, and Bers, 1963, and Stix, 1962]. In the CMA diagram, plasma parameter space is divided into closed volumes bounded by resonance and cutoff surfaces, and in each of the closed volumes the topological genera of the wave-normal surfaces are schematically illustrated. For the sake of simplicity a cold plasma consisting of electrons and one species of ions is assumed in the present paper. A brief summary of the dispersion relation and of the topology of wave-normal surfaces is given in sections 2.1 and 2.2.

For labeling modes the scheme proposed by Allis [1959] is adopted. In this scheme, modes are labeled "right-handed" or "left-handed" according to the polarization for the longitudinal propagation, and "ordinary" or "extraordinary" depending on whether the refractive index for the transverse propagation is independent or dependent on the magnetic field. As has been pointed out by Allis [1959] and Stix [1962], this labeling system avoids the confusion that can arise from the reversal of polarization at a certain angle of the wave-normal vector relative to the magnetic field within some of the bounded volumes in plasma parameter space, and also from different combinations of the two sets of the labels. The polarization reversal mentioned above is discussed in detail in section 2.5. In section 2.4, a CMA diagram for VLF to ULF waves and appropriate to the magnetosphere is presented, using the model magnetosphere described in section 2.3.

In sections 3.1 to 3.3 a formulation of general ray theory is presented without limitation on wave frequency, and in sections 3.4 to 3.8 the theory is applied to propagation of hydromagnetic waves in the magnetosphere. Analogy between the Hamiltonian form of classical mechanics and geometrical electromagnetics

¹Paper presented at the ULF Symposium, Boulder, Colo., 17 to 20 August 1964.

is demonstrated in sections 3.2 to 3.4, and validity of Fermat's principle is examined in section 3.3. The "action" is defined for a ray, and the principle of least action is established. It is then shown that if the dispersion relation is homogeneous in frequency ω and wave vector \mathbf{k} , the principle of least action implies the principle of least time, i.e., Fermat's principle. This result is the same as that obtained by Weinberg [1962] by the eikonal theory.

Formulating the ray theory in a Hamiltonian form, it is shown in section 3.5 that when the magnetic field and the plasma are axially symmetric the generalized momentum conjugate to the azimuthal coordinate is a constant of motion. Applying this result to the propagation of hydromagnetic waves in a model magnetosphere with a dipole magnetic field, "forbidden" and "allowed" regions for the ray are defined in the same manner as in Störmer's theory [1955] for a charged particle moving in a dipole field. It will be shown that because of the existence of a maximum in the Alfvén velocity at an altitude of several thousand kilometers above ground level, the accessibility of hydromagnetic rays generated in the outer region of the magnetosphere to the immediate vicinity of the earth is very limited.

When the magnetic field is not axially symmetric, the canonical equations must be integrated. In section 3.8 we will present examples of hydromagnetic ray trajectories on the equatorial plane which were computed by a numerical method for a model magnetosphere that takes into account the distortion of the dipole field due to the solar wind.

2. Propagation of Hydromagnetic Waves

2.1. Dispersion Relation

The dispersion relation for a two-component cold plasma in a uniform magnetic field is given by the following equation [Åström, 1950; Sitenko and Stepanov, 1957; Allis, 1959; and Stix, 1962; we follow this last author's representation]:

$$An^4 - Bn^2 + C = 0, \quad (1)$$

where n is the refractive index, and where A , B , and C are defined by:

$$A = S \sin^2 \theta + P \cos^2 \theta$$

$$B = RL \sin^2 \theta + PS (1 + \cos^2 \theta)$$

$$C = PRL$$

$$S = \frac{1}{2} (R + L)$$

$$R = 1 - \alpha / (1 + \Omega_i / \omega) (1 - \Omega_e / \omega)$$

$$L = 1 - \alpha / (1 - \Omega_i / \omega) (1 + \Omega_e / \omega)$$

$$P = 1 - \alpha$$

$$\alpha = (\pi_e^2 + \pi_i^2) / \omega^2$$

$\pi_{e,i}$ = electron or ion plasma frequency

$\Omega_{e,i}$ = electron or ion cyclotron frequency

ω = angular wave frequency

θ = angle between the wave normal and the magnetic field.

2.2. CMA Diagram for a Two-Component Cold Plasma

The CMA diagram with Ω_e^2 / ω^2 as ordinate and α as abscissa is shown in figure 1. To make the bounding curves reasonably well separated from each other, the ratio μ of the ion mass to the electron mass is taken to be 4 for illustrative purposes, as was done by Allis [1959] and Stix [1962]. In figure 1 the bounding curves are the electron cyclotron resonance ($R = \pm \infty$), the ion cyclotron resonance ($L = \pm \infty$), the upper and lower hybrid resonances ($S = 0$), and the cutoffs ($R = 0$, $L = 0$, and $P = 0$). The curve for $RL - PS = 0$ is also drawn with broken lines; this curve represents neither a cutoff nor a resonance, but it is found to be useful in labeling the modes [Stix, 1962].

For the longitudinal propagation ($\theta = 0$), the polarization in the electric field is circular in either a right-handed or left-handed sense. The wave-normal surfaces are labeled R or L on top of each sketch according as the polarization at $\theta = 0$ is right-handed ($n^2 = R$) or left-handed ($n^2 = L$), respectively. For the transverse propagation ($\theta = \pi/2$), wherever such propagation is possible, n^2 for one of the two branches is independent of the magnetic field ($n^2 = P$), and n^2 for the other branch depends on the magnetic field ($n^2 = RL/S$). The former branch is labeled with "0" for the ordinary mode, and the latter branch with "X" for the extraordinary mode. This system of labeling the mode seems to be most systematic and is recommended for general use to eliminate the confusion that existed in the past.

As we shall see in section 2.7, in an approximation for frequencies much less than the ion cyclotron frequency, the wave-normal surface for the mode labeled R and X in figure 1 becomes a sphere; that is n^2 is independent of θ . For this reason Åström [1950] called this mode "ordinary" and the other mode "extraordinary," and Åström's nomenclature has been used widely in the literature dealing with hydromagnetic waves. However, this labeling is not consistent with Allis's system, as was pointed out by Allis [1959] and Stix [1962]. Since the spherical wave-normal surface in question is merely an approximation, valid only for frequencies well below the ion cyclotron frequency, Allis's system is preferable. As is evident in figure 1, a right-handed (or left-handed) mode at $\theta = 0$ may be either an ordinary or extraordinary mode at $\theta = \frac{1}{2}\pi$, and thus labeling the modes with only one label, R or L , or 0 or X , is not adequate. Also, the polarization may reverse its direction in some of the modes, as was pointed out by Stix [1962]; this problem will be discussed in section 2.5.

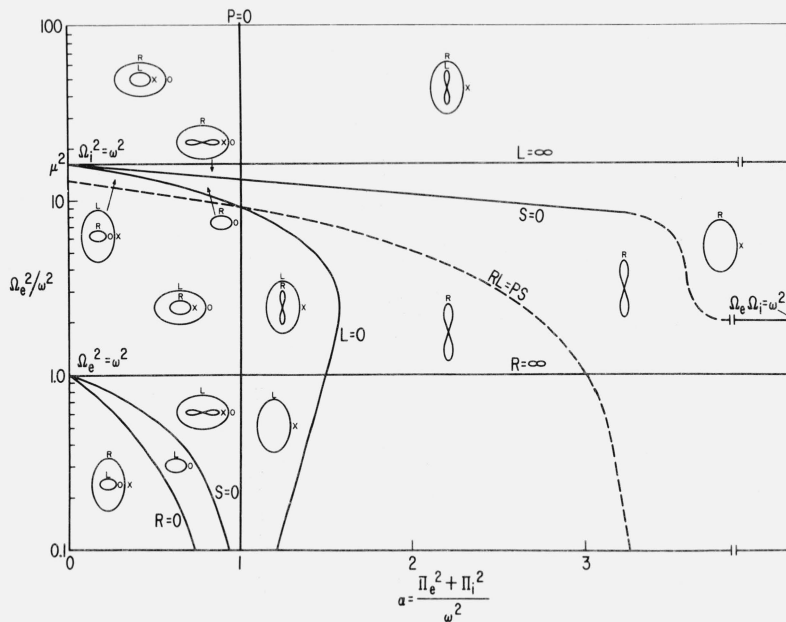


FIGURE 1. The CMA diagram for a two-component cold plasma, showing the topological characteristics of the wave-normal surfaces.

The two modes can be distinguished by still another labeling system. They can be labeled "fast" or "slow" according to the relative sizes of the wave-normal surfaces. There can be no crossing of the wave-normal surfaces for the two branches so that the labeling with fast or slow mode can be made unambiguously.

2.3. Model Magnetosphere

In section 2.4 a CMA diagram for ULF to VLF waves in the magnetosphere will be presented. The model magnetosphere to be used for the CMA diagram and also for the discussions of propagation of hydromagnetic waves in section 3 is described below.

We approximate the earth's magnetic field by a dipole field except in section 3.8 where the distortion of the dipole field by the solar wind is taken into account.

The electron density distribution in the magnetosphere adopted here is based on the recent determination by Liemohn and Scarf [1964] using nose whistlers. Among the electron density distributions which these authors considered to give self-consistent results, we adopt the simplest distribution; namely, the model in which the electron density is inversely proportional to the distance from the earth's center. Their results apply to the region of the magnetosphere from approximately 3 to 5 earth-radii. We assume that this inverse cube law for the electron density holds in regions below and above these altitudes. To be precise, we assume that the electron density varies as $N_0(a/r)^3$ on the equatorial plane from 15,000 km geocentric distance to the boundary of the magnetosphere, which is taken to be at $10a$; here a is the radius of the earth and N_0 is taken to be 1.41×10^4 electrons/cm³ [Liemohn and Scarf, 1964].

For altitudes below the bottom limit of the above distribution (15,000 km geocentric distance), we base our model on that given by Dessler, Francis, and Parker [1960], but to ensure continuity of the electron density an appropriate smoothing was made. In so doing, the region below 15,000 km was divided into two regions and in each region the electron density was expressed in a power series. At the boundary between the two regions and at 15,000 km geocentric distance, the electron density and its first derivative with respect to radial distance were made continuous. The density was expressed analytically for the convenience of the numerical calculations required later in the ray treatment.

Figure 2 shows the electron density distribution constructed in the manner described above and used throughout this paper. This distribution given in figure 2 refers to that in the equatorial plane, and we assume that the electron density is a function of radial distance alone.

2.4. CMA Diagram for ULF to VLF Waves in the Magnetosphere

Having obtained in section 2.2 the whole view of the CMA diagram for an idealized plasma in which the ion-to-electron mass ratio is taken to be 4, we now ask what regions in the plasma parameter plane are relevant to propagation of ULF to VLF waves in the magnetosphere. We will now take the actual value for the ratio of the hydrogen-ion mass to the electron mass.

In section 2.2 we took α and Ω_e^2/ω^2 as coordinates, but the conditions that are of interest to us now make it more convenient to use π_e/ω as abscissa and Ω_e/ω as ordinate. A CMA diagram for ULF to VLF with

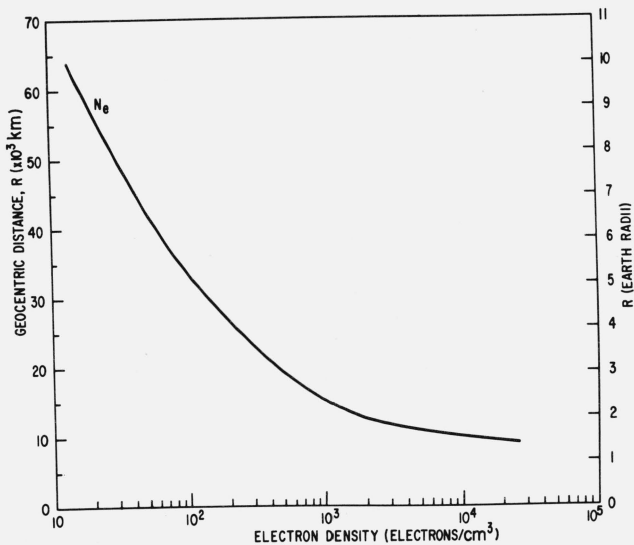


FIGURE 2. The electron density distribution in the model magnetosphere used in this paper.

drawn for frequencies from 0.01 Hz to 10 kHz. Since the plasma parameter variations with radial distance are the same for all frequencies, curves for different frequencies can be obtained from one of them by merely displacing it parallel to a fixed straight line. Since the magnetic field varies with latitude, the curves drawn in figure 3 for the equatorial plane will be changed at higher latitudes, but the changes are only slight because of the logarithmic scale in the diagram, and the general features which are discussed below will not be altered appreciably.

First we observe that for waves with frequencies below about 1 Hz, two modes are possible. One has a wave-normal surface topologically equivalent to a sphere; its electric field has right-handed circular polarization at $\theta=0$, and the mode is "extraordinary" at $\theta=\frac{1}{2}\pi$; this mode is the "fast" mode. The "slow" mode has a wave-normal surface topologically equivalent to a dumbbell-shaped lemniscoid, and its electric field has left-handed circular polarization at $\theta=0$. In the hydromagnetic approximation the former mode corresponds to Alfvén compressional wave and the latter to Alfvén shear wave. It is the latter mode that Alfvén [1942] originally derived by treating plasma as a conducting fluid.

In the frequency range from approximately 1 Hz to 100 Hz, the ion cyclotron resonance takes place at some altitude, and above this altitude only the fast mode can propagate. (We are concerned here only with altitudes above several hundred kilometers above ground level.)

For each frequency in the range from several tens of hertz to several kilohertz, the lower hybrid resonance (at $\theta=\frac{1}{2}\pi$, and $S=0$) is encountered at a certain altitude, and above that altitude the wave-normal surface is transformed to a dumbbell-shaped lemniscoid; propagation across the magnetic field becomes impossible. The mode prevailing at frequencies above the lower hybrid resonance frequency is the so-called "whistler" mode. Between the ion cyclotron frequency and the lower hybrid resonance frequency the propagation is not strongly guided along the magnetic field as in the whistler mode. This is due to the presence of ions, as was first pointed out by Hines [1957].

As we go to still higher frequencies we reach the electron cyclotron resonance, and the whistler mode also becomes impossible. If we cross the cutoff $L=0$ from right to left in figure 3, we have one or two modes, according as the frequency is above or below the electron cyclotron resonance.

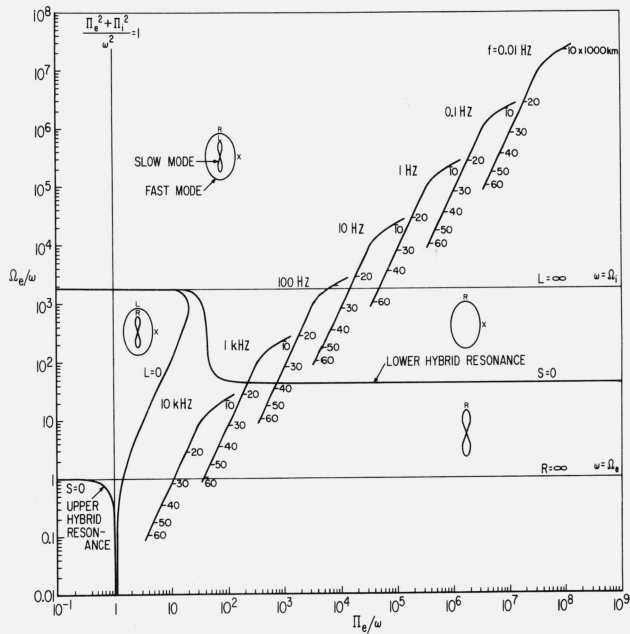


FIGURE 3. The CMA diagram for ULF and VLF waves in the model magnetosphere.

these coordinate axes is shown in figure 3. The diagram can be used in two ways. If the frequency ω is specified, the change in the plasma parameters with distance from the earth's center (for instance, on the equatorial plane) can be represented by a curve along which the radial distance is marked. Alternatively, if a position in the magnetosphere is specified, a continuous change in the wave frequency at that position can be represented by a continuous curve in the CMA diagram. For the sake of convenience we take the former representation. In figure 3, curves are

2.5. Polarization Reversal

In this section we examine polarization at θ not equal to zero. In section 2.2 we already mentioned the possibility of reversal of polarization. Stix [1962] showed that for one of the branches the polarization of the electric field is reversed at θ , satisfying the relation

$$\sin^2 \theta = P/S. \quad (2)$$

Clearly, for this reversal of polarization to take place for real θ , P and S must be of the same sign and $|P/S| \leq 1$. Even if these conditions are both satisfied, the reversal may occur in an evanescent branch. Thus it is worthwhile examining the problem in detail.

From the condition that P and S are of the same sign we can eliminate about one-half of the bounded areas in the CMA diagram. By the second condition; namely, that $|P/S| \leq 1$, part of the remaining areas are further eliminated. In figure 4, areas where polarization reversal cannot occur are shaded; signs of P and S are indicated by a small symbol + or -. The coordinates in figure 4 are the same as in figure 1, and the ion-to-electron mass ratio μ is again taken to be 4; this is just for schematical representation, and our discussion below applies to the case in which μ is the actual ion-to-electron mass ratio. The horizontal line at $\Omega_e^2/\omega^2 = \mu^2$ corresponds to $\Omega_i^2 = \omega^2$, i.e., the ion cyclotron resonance. Another horizontal line at $\Omega_e^2/\omega^2 = \mu^2 - \mu + 1$ plays an important role in the following discussions. This comes about from the fact that $P-S$ has the factor $\Omega_e^2/\omega^2 - (\mu^2 - \mu + 1)$ in the numerator. For $\mu > 1$, $\mu^2 > \mu^2 - \mu + 1 > 1$. It can be shown that $\mu^2 - \mu + 1$ is the ordinate (Ω_e^2/ω^2) for the intersection of $P=0$ and $S=0$, and that the curve $RL - PS = 0$ intersects the Ω_e^2/ω^2 axis at $\mu^2 - \mu + 1$. From figure 4 it is already clear that the reversal can never occur in the magnetosphere in waves with frequencies below the ion cyclotron frequency.

Next we examine in which branch the polarization reversal takes place, if it does at all, without limiting ourselves to the conditions of our immediate interest. By examining the polarization of the electric field it can be shown that if the polarization reversal occurs, it does so in one of the branches of n^2 in the following expression:

$$n^2 = (B \pm F)/(2A), \quad (3)$$

where

$$F^2 = (RL - PS)^2 \sin^4 \theta + P^2(R - L)^2 \cos^2 \theta.$$

It is found that if $RL + PS - 2S^2$ is negative, the reversal occurs in the branch coming from the positive sign in the above equation, and that if $RL + PS - 2S^2$ is positive, the reversal occurs in the other branch.

It is, therefore, instructive to locate the solution to the equation

$$RL + PS - 2S^2 = 0. \quad (4)$$

The left-hand side of (4) can be written as follows:

$$\begin{aligned} & RL + PS - 2S^2 \\ &= -\alpha x^2(\mu^2 - x^2)^{-2}(1 - x^2)^{-2} [x^6 - \{2\mu^2 - (1 + \alpha)\mu + 2\} x^4 \\ & \quad + \{\mu^4 - (1 + \alpha)\mu^3 + 3\mu^2 - (1 + \alpha)\mu + 1\} x^2 \\ & \quad - \mu^2\{(1 - 2\alpha)\mu^2 - (1 - 3\alpha)\mu + 1 - 2\alpha\}], \quad (5) \end{aligned}$$

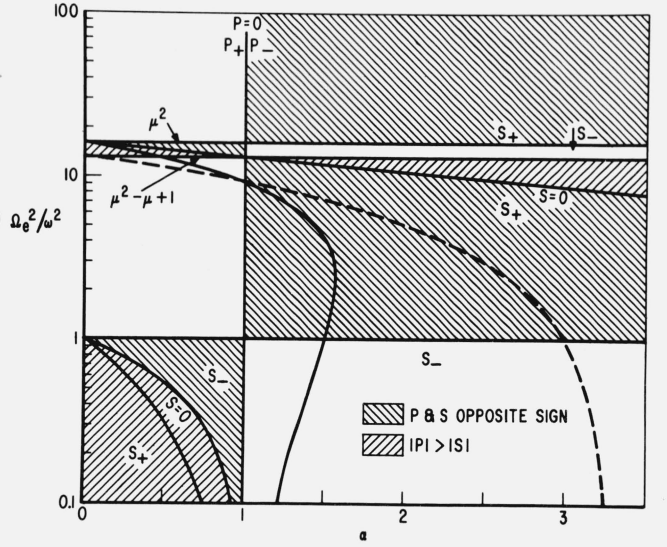


FIGURE 4. Areas in the plasma parameter plane in which the polarization reversal can occur at θ satisfying (2).

where

$$x = \Omega_e/\omega.$$

The expression on the right-hand side of (5) can also be written as

$$\begin{aligned} & -\alpha x^2(\mu^2 - x^2)^{-2}(1 - x^2)^{-2} [(x^2 - \mu^2) \\ & \quad \{x^2 - (\mu^2 - \mu + 1)\}(x^2 - 1) + \alpha\mu\{(x^2 - \mu^2) \\ & \quad \quad (x^2 - 1) + 2\mu(\mu - 1)^2\}]. \end{aligned}$$

Though the latter expression is convenient to determine α when x^2 is given, we will use (5) to obtain the solution to (4). From (5) we see that $x^2 = 0$ is a solution of (4), which, however, is of no interest to us.

We now examine the solution of the equation that is obtained by equating the content of the square brackets in (5) to zero. Since the equation so obtained is cubic in x^2 , we can determine the number of real roots by examining the discriminant. This method is helpful in locating the solutions.

For $\alpha \gg \mu$ and x^2 not very much greater in order of magnitude than μ , x^2 becomes independent of α , and we have two positive roots:

$$x^2 = \mu^2(1 - 2/\mu), \text{ or } 2\mu,$$

thus giving two positive roots for x

$$x = \mu(1 - 2/\mu)^{1/2}, \text{ or } (2\mu)^{1/2}.$$

Numerically, these are approximately 1835.50 and 60.64, respectively. There are three positive real roots for positive α less than 0.175. Between 0.175 and 5.835 there is only one negative real root. For α greater than 5.835 there are two positive real roots and one negative real root. (The numbers quoted are accurate to ± 0.005 .)

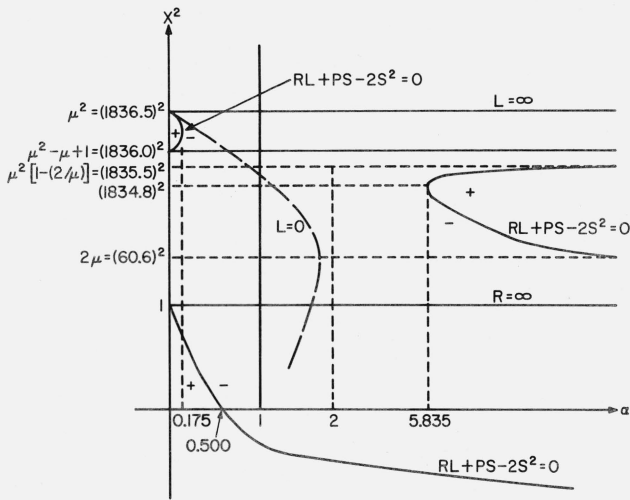


FIGURE 5. Illustrating the solutions to $RL + PS - 2S^2 = 0$.

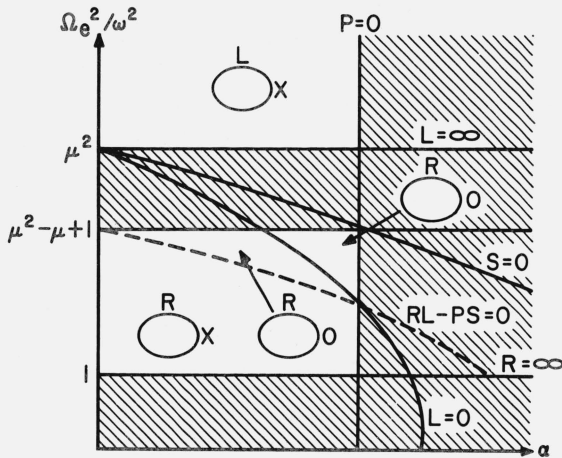


FIGURE 6. The modes in which polarization reversal occurs at θ satisfying (2).

The curves representing (4) are schematically shown in figure 5; the sign for $RL + PS - 2S^2$ is also indicated for areas separated by the curves.

We now combine the results in figures 4 and 5. In so doing we observe that the intersection of $R = \infty$ and $L = 0$ is at $\alpha = 2(1 - 1/\mu) < 2$. We see that all the unshaded areas in figure 4 where the polarization reversal can occur are in the regions where $RL + PS - 2S^2$ is negative. Thus the reversal occurs in the branch resulting from the plus sign in (3).

We reach the conclusion that there is no polarization reversal in the nonevanescant modes to the right of the vertical line $\alpha = 1$, and that for α less than 1 the polarization reversal occurs in the $L-X$ mode for $\omega^2 < \Omega_i^2$ and in the $R-0$ or $R-X$ mode for $\Omega_i^2(1 - 1/\mu + 1/\mu^2) < \omega^2 < \Omega_e^2$.

The modes in which the polarization reversal occurs are indicated in figure 6, which summarizes the

discussions given above. We conclude that for ULF to VLF waves in the magnetosphere, the polarization reversal at θ satisfying (2) does not occur.

2.6. Lower Hybrid Resonance

For propagation across the magnetic field, i.e., for $\theta = \frac{1}{2}\pi$, there is a resonance at $S = 0$. As is indicated in figures 1 and 3, there are two such resonances, and the one at the lower frequency is called the lower hybrid resonance and the other the upper hybrid resonance.

Approximate expressions for the two hybrid resonance frequencies can be obtained by ignoring terms of order μ^{-1} compared with unity in the dispersion relation for $\theta = \frac{1}{2}\pi$. Stix [1962] gives for the lower hybrid resonance frequency ω_{LH} ,

$$1/\omega_{LH}^2 = 1/(\Omega_i^2 + \pi_i^2) + 1/\Omega_i\Omega_e, \quad (6)$$

and for the upper hybrid resonance frequency ω_{UH} ,

$$\omega_{UH}^2 = \Omega_e^2 + \pi_e^2. \quad (7)$$

In the frequency range we are concerned with here and for the plasma parameters appropriate to the magnetosphere, the lower hybrid resonance frequency can be approximated with good accuracy by the geometric mean of the ion and electron cyclotron frequencies:

$$\omega_{LH} = (\Omega_i\Omega_e)^{1/2}. \quad (8)$$

A clear physical picture for this resonance has been given by Auer, Hurwitz, and Miller [1958].

The lower hybrid resonance frequency at different distances from the earth's center is given in table 1 for the model magnetosphere used in this paper.

TABLE 1. The lower hybrid resonance frequency f_{LH} at various distances from the center of the earth

r	f_{LH}
<i>km</i>	<i>Hz</i>
10,000	5,260
15,000	1,560
20,000	657
25,000	337
30,000	195
35,000	123
40,000	82
45,000	58
50,000	42
55,000	32
60,000	24

2.7. Hydromagnetic Approximation

When the wave frequency ω is well below the ion cyclotron frequency Ω_i , the quantities R and L are simplified, and both R and L can be approximated by $1 + \gamma$, where $\gamma = 4\pi\rho c^2/B_0^2$; here $\rho = n_i m_i + n_e m_e$, i.e., the plasma density. With this approximation for R and L the dielectric tensor becomes diagonal. The

component K_{\perp} of the dielectric tensor perpendicular to the magnetic field then takes the well-known form [Spitzer, 1956],

$$K_{\perp} = 1 + \gamma.$$

If α is large, as is the case with ULF waves in the magnetosphere, P can be approximated by $-\alpha$. With these approximations for R , L , and P , the dispersion relation is simplified and readily factored, giving the following two modes. One of these modes gives

$$n^2 = 1 + \gamma, \quad (9)$$

and the other

$$n^2 \cos^2 \theta = 1 + \gamma. \quad (10)$$

In the first mode, n^2 is independent of θ . For this reason Åström [1950] called this mode "ordinary" mode, and the second "extraordinary" mode. However, a closer examination shows that the first mode corresponds to the branch labeled $R-X$ in figure 3 and the second to that labeled L . Hence the exact expression for n^2 for the first mode depends on the magnetic field for $\theta = \frac{1}{2}\pi$. The problem of labeling the modes has already been discussed in section 2.2.

By studying the ion velocity, the mode corresponding to (9) can be shown to represent *compressional* wave, and the other mode (10) *shear* wave. From a comparison of phase velocity for these two modes, one finds that the compressional mode is the fast mode and that the shear mode is the slow mode.

From the continuity of the wave-normal surface we see that the Alfvén compressional mode (or the fast hydromagnetic mode) and the whistler mode belong to the same family. The Alfvén shear mode (or the slow hydromagnetic mode) disappears at the ion cyclotron frequency.

When $\gamma \gg 1$, the phase velocities for the compressional and shear modes reduce to V_A and $V_A \cos \theta$, respectively, where $V_A = B_0 / \sqrt{4\pi\rho}$, which is the Alfvén velocity. The condition that $\gamma \gg 1$ is equivalent to the condition that $V_A/c \ll 1$. These approximations for the phase velocities can be readily obtained by a fluid-dynamical treatment of plasma with infinite conductivity and by neglecting displacement current.

3. Ray Theory

3.1. Introduction

So far we have reviewed the wave modes in a cold plasma by studying the wave-normal surfaces. The basis for the study was the dispersion relation. We now investigate propagation of hydromagnetic waves from a somewhat different angle by constructing a ray theory. As the plane wave theory described in the preceding discussions has limitations in its application, the ray theory developed below is valid only under certain conditions. However, just as the general discussions of wave modes are useful in understanding

the propagation of waves, the theoretical study of the behavior of rays is helpful in understanding some of the electromagnetic phenomena occurring in the magnetosphere.

Although the theoretical discussions in sections 3.2 and 3.3 are of general nature, the theory is applied in sections 3.4 to 3.8 to propagation of hydromagnetic waves in the magnetosphere.

3.2. Equations of Motion of a Ray

The basis of the theory is that the ray propagates with group velocity. Hines [1951] and Auer, Hurwitz, and Miller [1958] have shown that the constructive interference maximum of a wave packet moves with group velocity. We also assume that the waves constituting the wave packet propagate in the same mode throughout its motion in the anisotropic medium. Coupling between different modes is assumed not to take place.

Denoting the position of a ray by \mathbf{r} and the group velocity by \mathbf{v}_g , we write the equation of motion for the ray as follows:

$$\dot{\mathbf{r}} = \mathbf{v}_g, \quad (11)$$

where the dot signifies differentiation with time t . The group velocity \mathbf{v}_g is given by

$$\mathbf{v}_g = \partial\omega / \partial\mathbf{k}. \quad (12)$$

The wave frequency ω and the wave vector \mathbf{k} are related by the dispersion relation, which we write

$$D(\mathbf{k}, \omega, \mathbf{r}, t) = 0. \quad (13)$$

We introduce a parameter τ along the path of the ray. Then, using (12) and (13), the equation of motion (11) can be written in the following form:

$$\frac{d\mathbf{r}/d\tau}{dt/d\tau} = - \frac{\partial D / \partial \mathbf{k}}{\partial D / \partial \omega}. \quad (14)$$

From our assumption D is constant along the trajectory, and hence we have

$$\delta D = \left(\frac{\partial D}{\partial \mathbf{k}} \cdot \frac{d\mathbf{k}}{d\tau} + \frac{\partial D}{\partial \omega} \frac{d\omega}{d\tau} + \frac{\partial D}{\partial \mathbf{r}} \cdot \frac{d\mathbf{r}}{d\tau} + \frac{\partial D}{\partial t} \frac{dt}{d\tau} \right) = 0. \quad (15)$$

For (15) to hold for any τ the content of the parentheses must be zero. We group the four terms in the parentheses in (15) as follows:

$$\left(\frac{\partial D}{\partial \mathbf{k}} \cdot \frac{d\mathbf{k}}{d\tau} + \frac{\partial D}{\partial \mathbf{r}} \cdot \frac{d\mathbf{r}}{d\tau} \right) + \left(\frac{\partial D}{\partial \omega} \frac{d\omega}{d\tau} + \frac{\partial D}{\partial t} \frac{dt}{d\tau} \right) = 0. \quad (16)$$

If each of the two factors in (16) is zero, the required condition (15) is satisfied. Equations (14) and (16)

are satisfied by the following set of equations:

$$d\mathbf{r}/d\tau = \partial D/\partial \mathbf{k} \quad (17)$$

$$d\mathbf{k}/d\tau = -\partial D/\partial \mathbf{r} \quad (18)$$

$$dt/d\tau = -\partial D/\partial \omega \quad (19)$$

$$d\omega/d\tau = \partial D/\partial t \quad (20)$$

If D is independent of time, the last equation (20) states that ω is conserved along the ray trajectory. The third equation (19) gives the relation between time t and parameter τ .

The above set of equations clearly indicates an analogy between the ray theory and classical mechanics. The wave vector \mathbf{k} and the frequency ω of a ray play the roles of the momentum and the energy of a particle, respectively. However, this analogy does not enable us to formulate the ray theory in Hamiltonian form. This is because the motion of a ray corresponds to that of a particle of zero mass, and hence it is expected that the Lagrangian for the ray is identically zero. In the conclusion of section 3.3 we will show that the Lagrangian indeed vanishes.

However, when Fermat's principle is valid the problem can be formulated in Hamiltonian form. Hence we now examine under what conditions Fermat's principle is consistent with our formulation.

3.3. Fermat's Principle

Weinberg [1962] showed that when the *eikonal* is stationary, the principle of least time, i.e., Fermat's principle, holds if the dispersion relation is homogeneous in \mathbf{k} and ω . Here we derive the same condition by pursuing the formulation in section 3.2.

In classical mechanics the principle of least action holds when the Hamiltonian is conserved. We limit ourselves to the case when the frequency ω is conserved along the path, that is, D is conserved along the path.

We first define the action A for the ray by the integral

$$A = \int_{t_1}^{t_2} \mathbf{k} \cdot \dot{\mathbf{r}} dt \quad (21)$$

where the dot means, as before, differentiation with t .

Next, we calculate the variation ΔA , where the Δ -variation differs from the δ -variation appearing in virtual displacement; in the latter, time is kept unchanged, whereas in the former the process involves a change dt [see, e.g., Goldstein, 1951]. For any function f of \mathbf{r} and t , the Δ -variation of f is

$$\begin{aligned} \Delta f &= d\tau \left(\frac{\partial f}{\partial \tau} + \dot{f} \frac{dt}{d\tau} \right) \\ &= \delta f + \dot{f} \Delta t. \end{aligned} \quad (22)$$

In particular,

$$\Delta \mathbf{r} = \delta \mathbf{r} + \dot{\mathbf{r}} \Delta t. \quad (23)$$

Applying the Δ -variation to (21) we have

$$\Delta A = \int_{t_1}^{t_2} \delta(\mathbf{k} \cdot \dot{\mathbf{r}}) dt + \mathbf{k} \cdot \dot{\mathbf{r}} \Delta t \Big|_{t_1}^{t_2} \quad (24)$$

The first integral can be calculated in the following way:

$$\begin{aligned} \int_{t_1}^{t_2} \delta(\mathbf{k} \cdot \dot{\mathbf{r}}) dt &= \int_{t_1}^{t_2} \delta \mathbf{k} \cdot \dot{\mathbf{r}} dt + \int_{t_1}^{t_2} \mathbf{k} \cdot \delta \dot{\mathbf{r}} dt \\ &= \int_{t_1}^{t_2} \delta \mathbf{k} \cdot \dot{\mathbf{r}} dt - \int_{t_1}^{t_2} \dot{\mathbf{k}} \cdot \delta \mathbf{r} dt + \mathbf{k} \cdot \delta \mathbf{r} \Big|_{t_1}^{t_2} \\ &= \int_{t_1}^{t_2} (\delta \mathbf{k} \cdot \dot{\mathbf{r}} - \dot{\mathbf{k}} \cdot \delta \mathbf{r}) dt - \mathbf{k} \cdot \dot{\mathbf{r}} \Delta t \Big|_{t_1}^{t_2}. \end{aligned}$$

Here we used the fact that the order of the δ - and dot-operation can be interchanged, and partial integration was performed on the second integral on the right-hand side of the first line. To obtain the last result we used (23) and the condition that $\Delta r = 0$ at the end points.

Thus (24) reduces to

$$A = \int_{t_1}^{t_2} (\delta \mathbf{k} \cdot \dot{\mathbf{r}} - \dot{\mathbf{k}} \cdot \delta \mathbf{r}) dt.$$

Using (11), (12), (17), (18), and (19), the integrand can be transformed as follows:

$$\begin{aligned} \delta \mathbf{k} \cdot \dot{\mathbf{r}} - \dot{\mathbf{k}} \cdot \delta \mathbf{r} &= -(\partial D/\partial \omega)^{-1} \left(\delta \mathbf{k} \cdot \frac{\partial D}{\partial \mathbf{k}} + \delta \mathbf{r} \cdot \frac{\partial D}{\partial \mathbf{r}} \right) \\ &= -(\partial D/\partial \omega)^{-1} \delta D \\ &= 0. \end{aligned}$$

Thus we have proved that

$$\Delta A = 0.$$

Namely, in our system the principle of least action holds if the action is defined by (21). Having proved this principle we go back to the expression for ΔA given in (24). If

$$\mathbf{k} \cdot \dot{\mathbf{r}} = \text{constant} \neq 0, \quad (25)$$

then (24) reduces to

$$\Delta(t_2 - t_1) = 0$$

which implies the principle of least time, or Fermat's

principle. The condition (25) can be rewritten as follows:

$$-(\mathbf{k} \cdot \partial D / \partial \mathbf{k}) / (\partial D / \partial \omega) = \text{constant}. \quad (26)$$

A sufficient condition for (26) to hold is that D is homogeneous in \mathbf{k} and ω , because if D is homogeneous in \mathbf{k} and ω , i.e., if

$$D(\alpha \mathbf{k}, \alpha \omega) = \alpha^n D(\mathbf{k}, \omega),$$

Euler's homogeneity equation becomes

$$\mathbf{k} \cdot \frac{\partial D}{\partial \mathbf{k}} + \omega \frac{\partial D}{\partial \omega} = nD = 0. \quad (27)$$

Thus the constant in (26) takes the value of ω .

The homogeneity equation (27) can be transformed into the form

$$\mathbf{v}_g \cdot \frac{\mathbf{k}}{\omega} = 1 \quad \text{or} \quad \frac{\partial \omega}{\partial |\mathbf{k}|} = \frac{\omega}{|\mathbf{k}|}$$

which implies the equality of the phase velocity and the component of the group velocity in the direction of the former.

It is pointed out here that the action (21) is the same as the eikonal S in Weinberg's formulation, and that the principle of least action derived here is equivalent to the principle of stationary S in Weinberg's eikonal theory.

For the Alfvén compressional mode the dispersion relation is homogeneous in \mathbf{k} and ω , and hence Fermat's principle holds. As a matter of fact, for this mode the group velocity is equal to the phase velocity. However, for the shear mode the dispersion relation is not homogeneous in the components of \mathbf{k} , and thus Fermat's principle does not hold. As has been noted by Weinberg [1962], the application of Fermat's principle by Francis, Green, and Dessler [1959] is justified.

In concluding this section a remark is made on the Lagrangian. In classical mechanics the Lagrangian L is related to the Hamiltonian by

$$L = \mathbf{p} \cdot \dot{\mathbf{r}} - H$$

where \mathbf{p} is the momentum.

If we define the Lagrangian for the ray by

$$L = \mathbf{k} \cdot \dot{\mathbf{r}} - \omega$$

then from (25) our Lagrangian is identically zero, confirming our expectation expressed in section 3.2. Thus the ray theory cannot be constructed in Hamiltonian form using the Lagrangian defined above.

3.4. Ray Theory for Modes With Isotropic Phase Velocity

In this and in the following sections we discuss the case in which the phase velocity is isotropic. We specifically study propagation of a hydromagnetic

ray. For the Alfvén compressional mode the group velocity is the same as the phase velocity. Hence we simply refer to these velocities by the single term the Alfvén velocity.

Fermat's principle states that the motion of a ray from a point P_1 to another point P_2 is such that the

variation of the line integral $\int_{P_1}^{P_2} ds/V$ for fixed P_1 and P_2 is zero, i.e.,

$$\delta \int_{P_1}^{P_2} ds/V(r, \theta, \phi) = 0 \quad (28)$$

where $V(r, \theta, \phi)$ is the Alfvén velocity, using a spherical coordinate system (r, θ, ϕ) . When we refer to the magnetosphere the origin of the spherical coordinate system is taken to coincide with the earth's center. In the preceding sections θ was the angle which \mathbf{k} makes with the magnetic field, but in the rest of the paper θ is the polar angle.

We write (28) in the form:

$$\delta \int_{t_1}^{t_2} \frac{(\dot{r}^2 + r^2 \dot{\theta}^2 + r^2 \dot{\phi}^2 \sin^2 \theta)^{1/2}}{V(r, \theta, \phi)} dt = 0 \quad (29)$$

where t_1 and t_2 are the times when the ray is at P_1 and P_2 , and where the dot means differentiation with respect to time t .

Equation (29) is formally the same as the variation equation expressing Hamilton's principle for a system whose Lagrangian is equal to the integrand in (29). Thus we take the integrand of (29) as the Lagrangian of our system, and define the generalized momenta conjugate to r, θ, ϕ by

$$p_k = \partial L / \partial \dot{q}_k \quad (k = 1, 2, 3)$$

where it is understood that the subscript k refers to r, θ, ϕ components and that $q_k (k = 1, 2, 3)$ represents r, θ, ϕ , respectively.

The Hamiltonian H of the system is

$$\begin{aligned} H &= \sum_k p_k \dot{q}_k - L \\ &= V(r, \theta, \phi)^2 [p_r^2 + p_\theta^2 / r^2 + p_\phi^2 / (r^2 \sin^2 \theta)] - 1. \end{aligned}$$

Then the canonical equations can readily be formed. Stegelmann and von Kenschitzki [1964] proceeded to integrate the canonical equations numerically.

3.5. Axially Symmetric Case: Allowed and Forbidden Regions for a Ray

It is obvious that if the Alfvén velocity is independent of ϕ , the Hamiltonian does not contain ϕ explicitly; thus, ϕ is a *cyclic* coordinate. It follows that the conjugate momentum p_ϕ is a constant of motion. From the definition of p_ϕ , we immediately obtain the equation

$$(r^2 \dot{\phi} \sin^2 \theta) / V(r, \theta)^2 = \text{constant}. \quad (30)$$

This equation, of course, is the canonical equation for ϕ with p_ϕ constant.

Since $\dot{\phi} = V d\phi/ds$, where s is path length along the trajectory, (30) can be written as follows:

$$(R^2/V)d\phi/ds = \alpha \quad (31)$$

where

$$R = r \sin \theta \quad (32)$$

and where α is a constant.

We define an angle χ by the equation

$$R d\phi/ds = \sin \chi \quad (33)$$

so that χ is the angle between the tangent to the ray in the direction of its motion and the meridian plane. As can be seen in (33) the sign of χ is taken such that χ is positive when ϕ increases as the ray advances. Figure 7 illustrates the angle χ .

Using χ , (31) reduces to

$$(R/V) \sin \chi = \alpha. \quad (34)$$

For rays belonging to α , (34) gives the angle χ as a function of r and θ .

Since $-1 \leq \sin \chi \leq 1$, we have the relation

$$-1 \leq \alpha V/R \leq 1. \quad (35)$$

Thus, given the value of α , (35) defines the "allowed" region for the rays belonging to α . Areas outside the allowed region are forbidden to these rays.

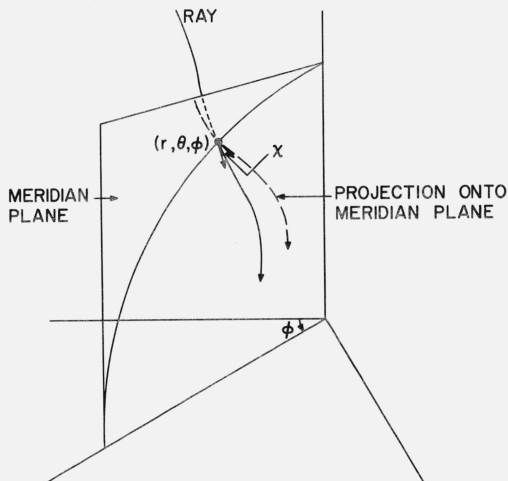


FIGURE 7. Illustrating the angle χ .

The constant α can be taken as the initial condition specified by r_0 , θ_0 , and χ_0 :

$$\alpha = (R_0/V_0) \sin \chi_0 \quad (36)$$

where R_0 and V_0 are the values of R and V at r_0 , θ_0 .

It should be noted that the angle χ_0 does not specify the initial direction of a ray completely, except in the equatorial plane. To specify the initial direction of a ray completely one more angle is needed (sec. 3.8); however, we only need χ_0 for the time being.

When the initial conditions r_0 , θ_0 , and χ_0 are given, the *allowed* and *forbidden regions* can be mapped out using (35) without integrating the equations of motion.

The problem is formally identical with that in Störmer's work on the motion of a charged particle in a dipole magnetic field [Störmer, 1955]. In Störmer's problem the Hamiltonian for the particle does not contain ϕ explicitly.

The meaning of (33) becomes more explicit if we limit ourselves to rays confined in the equatorial plane. The Alfvén velocity V is now a function of r alone, and χ is the angle which the tangent to the ray trajectory makes with the radial direction. Let χ be measured positively from the inward radial direction toward the direction of increasing ϕ (which is taken to be eastward) and let χ vary from $-\pi$ to π ; thus rays with $-\frac{1}{2}\pi < \chi < \frac{1}{2}\pi$ are inbound and those with $|\chi| > \frac{1}{2}\pi$ are outbound, and when $\chi = \pm \frac{1}{2}\pi$, a ray is tangent to the circle of radius r .

The angle χ at r is related to its initial value χ_0 at the point source at r_0 by

$$\sin \chi = (r_0/r) (V/V_0) \sin \chi_0.$$

If $V(r)$ is a maximum at $r = r_m$ and is a monotonically decreasing function of r with increasing r , then for $r_0 > r > r_m$, the inequality $|\chi| > |\chi_0|$ always holds. This simply implies the obvious result that the ray is bent away from the region of high Alfvén velocity.

The Alfvén velocity is a maximum at several thousand kilometers altitude and decreases both above and below this level [Dessler, 1958]. The Alfvén velocity increases again near the F_2 peak, but we are not concerned here with the propagation of hydromagnetic waves in the ionosphere. We only consider the ray trajectories above 600 km altitude.

It is of interest to find the critical initial angle $\chi_{0,c}$ at which an inbound ray from a point source at a great distance is reflected away from the earth at the region ($r = r_m$) of the Alfvén velocity maximum. This critical initial angle can be determined by

$$|\sin \chi_{0,c}| = (r_m/r_0) (V_0/V_m)$$

where V_m is the value of V at r_m .

For a rough estimate, taking $r_0 = 60,000$ km, $r_m = 10,000$ km, and $V_0 = 400$ km/sec, $V_m = 2,000$ km/sec, we obtain $|\sin \chi_{0,c}| = 1/30$, and hence $|\chi_{0,c}|$ is about 1.9° . There are uncertainties in the distribution of Alfvén velocity in the magnetosphere, but $\chi_{0,c}$ is not

likely to be changed greatly as more accurate information on the Alfvén velocity distribution becomes available.

3.6. Further Remark on Ray Tracing in the Equatorial Plane

In 3.5, time t was used for the variable in the variation equation. However, any one of the three coordinates can be used as the variable in place of t .

If we choose ϕ as the variable, and if we confine ourselves to the equatorial plane, the integrand L in the variation equation reduces to

$$L(r, r') = (r'^2 + r^2)^{1/2} / V(r)$$

where the prime represents differentiation with respect to ϕ .

Considering this function as the Lagrangian, Lagrange's equation of motion is

$$\frac{d}{d\phi} \left(\frac{\partial L}{\partial r'} \right) - \frac{\partial L}{\partial r} = 0.$$

This is the equation used by Francis, Green and Dessler [1959].

Denoting the momentum conjugate to r by p , the Hamiltonian for the system is given by

$$H = pr' - L$$

where

$$p = \partial L / \partial r'.$$

It is understood that H is expressed as a function of r and p . Then the Hamiltonian does not contain ϕ explicitly. Thus the Hamiltonian is a constant of motion. We immediately arrive at the equation:

$$r' \frac{\partial L}{\partial r'} - L = \text{constant}.$$

This is the equation which Francis, Green, and Dessler [1959] derived mathematically and used for their calculation of the transit time for the ray, and which Dessler, Francis, and Parker [1960] used for their two dimensional ray tracing.

3.7. Hydromagnetic Rays in the Magnetosphere: Axially Symmetric Case

Using the method described in section 3.5, we will now investigate the accessibility of hydromagnetic rays originating from the magnetospheric boundary to the vicinity of the earth. We use the same model magnetosphere as the one presented in section 2.3; for the magnetic field we approximate the geomagnetic field by a centered dipole.

As was shown in section 3.5, when the position (r_0, θ_0) of the point source and the initial value of χ

of the ray are specified, we can determine the allowed and forbidden regions by (35) and (36).

We place the point source at the distance of 10 earth-radii from the earth's center, i.e., $r_0 = 10a$, where a is the earth's radius, and we determine allowed and forbidden regions for $\theta_0 = 30^\circ, 60^\circ, \text{ and } 90^\circ$; the last value of θ_0 places the source on the equatorial plane.

Typical diagrams showing the allowed and forbidden regions are presented in figure 8. In the figure, forbidden regions are indicated by patches and the open areas represent allowed regions. The patched circle in the center represents the earth and the position of the point source can be at any of the four arrows on the great circle whose radius is ten times that of the earth. All the diagrams are symmetric with respect to the equator, and the three dimensional allowed (or forbidden) region can be obtained by rotating each diagram about the vertical axis through the center, namely, the dipole axis.

For very small values of χ_0 (well below 1° , say), that is when the initial direction of the ray deviates from the meridian plane only by a small angle, the ray can reach the earth's vicinity except directly above the poles. As χ_0 increases, the two forbidden regions around the axis, one in each hemisphere, become larger and extend to lower latitudes near the altitude of the Alfvén velocity maximum. When χ_0 reaches some critical value, the tips of the northern and southern forbidden regions touch each other on the equatorial plane. There is an allowed region between the ionosphere and the altitude at which the two forbidden regions join on the equatorial plane, but this inner allowed region is not accessible to the ray coming from outside.

When χ_0 exceeds a certain value a little greater than the critical value, the earth is completely immersed in a forbidden region and the outer allowed region is more and more pushed outward, and finally, as χ_0 tends to 90° the inner surface of the outer allowed region approaches some limiting surface which intersects the large sphere (of radius r_0) at $\theta = \theta_0$ and $\theta = \pi - \theta_0$. When θ_0 is 90° , the allowed region for $\chi_0 = 90^\circ$ degenerates to a circle of radius r_0 on the equatorial plane.

The critical value of χ_0 becomes smaller as θ_0 increases; for $\theta_0 = 30^\circ, 60^\circ, \text{ and } 90^\circ$, the critical χ_0 is $3.3^\circ, 1.4^\circ, \text{ and } 0.9^\circ$, respectively. In figure 8 the diagrams for these critical circumstances are included. For $\chi_0 = 10^\circ, 30^\circ, 60^\circ, \text{ and } 90^\circ$ the forbidden regions are indicated in one diagram for each θ_0 .

We conclude that the earth and its immediate vicinity are remarkably well protected from the hydromagnetic rays generated in the outer regions of the magnetosphere. This feature has been shown by Stgelmann and von Kenschitzki [1964] with their results from numerical ray tracing.

3.8. Hydromagnetic Rays in the Distorted Magnetosphere: Axially Asymmetric Case

The magnetosphere is contained in a cavity in the streaming solar plasma [Cahill and Amazeen, 1963;

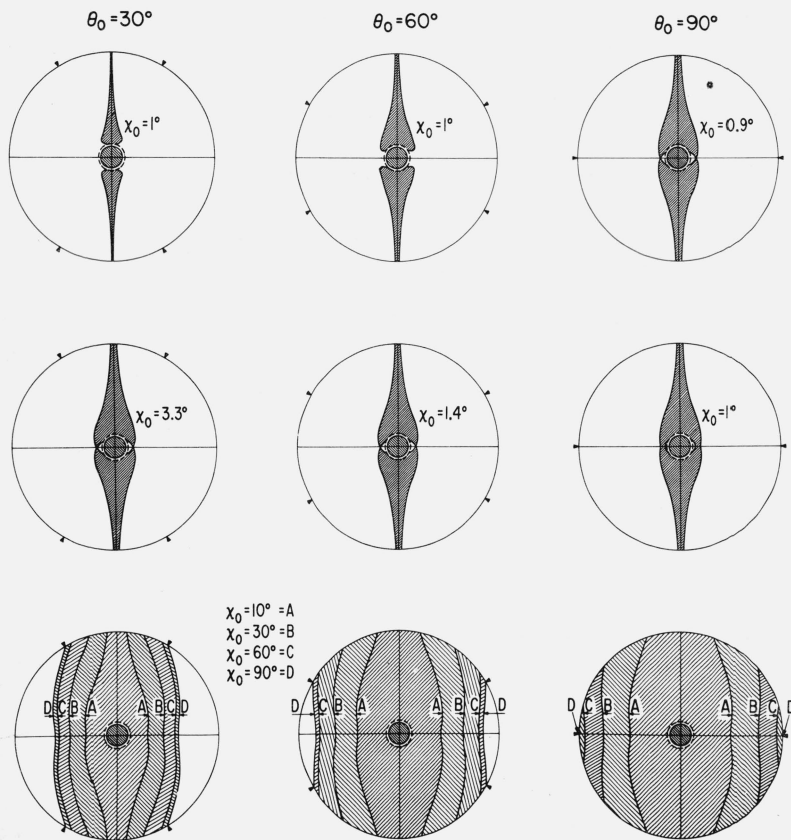


FIGURE 8. Allowed and forbidden regions for a hydromagnetic ray in the magnetosphere with a dipole field.

Ness et al., 1964]. A number of workers have attempted to theoretically determine the shape of the boundary of the magnetosphere [for reference, see a review paper by Beard, 1964]. In this section we only briefly discuss the effect of the distortion of the magnetosphere on the propagation of hydromagnetic waves.

In the absence of symmetry we have to write down the equations of motion and solve them by some numerical method. For the sake of convenience we multiply the Hamiltonian given in section 3.4 by the factor $\frac{1}{2}$. With this Hamiltonian the canonical equations are

$$\begin{aligned}
 \dot{r} &= V^2 p_r \\
 \dot{\theta} &= V^2 p_\theta / r^2 \\
 \dot{\phi} &= V^2 p_\phi / (r^2 \sin^2 \theta) \\
 \dot{p}_r &= -(1/V) \partial V / \partial r + (V^2 / r^3) (p_\theta^2 + p_\phi^2 / \sin^2 \theta) \\
 \dot{p}_\theta &= -(1/V) \partial V / \partial \theta + (V^2 / r^2) p_\phi^2 \cos \theta / \sin^3 \theta \\
 \dot{p}_\phi &= -(1/V) \partial V / \partial \phi.
 \end{aligned}
 \tag{37}$$

These equations are not completely independent. The Hamiltonian of the system is identically zero, and we have

$$p_r^2 + p_\theta^2 / r^2 + p_\phi^2 / (r^2 \sin^2 \theta) = 1 / V^2. \tag{38}$$

Using (38) one of the variables can be eliminated from the set of equations (37). But it is found convenient to use (38) as a check in the numerical ray tracing calculation.

We define the direction of the tangent to the ray trajectory at a point P by two angles χ and η . The angle χ is the same as that defined in the preceding section, and η is the angle which the tangent to the projection of the trajectory onto the meridian plane makes with the radial direction, namely

$$\begin{aligned}
 \sin \chi &= (d\phi/ds) r \sin \theta \\
 \cos \eta &= -(dr/ds) \sec \chi.
 \end{aligned}$$

We denote the initial values of χ and η at (r_0, θ_0, ϕ_0) by χ_0 and η_0 , respectively. The initial values of the momenta can be written in terms of $r_0, \theta_0, \phi_0, \chi_0, \eta_0$, and $V(r_0, \theta_0, \phi_0)$.

For the deformed geomagnetic field we take the model proposed by Mead [1964]. For the dipole field we take $g_1^0 = -0.31$ gauss, and for the additional field due to the deformation we take

$$\bar{g}_1^0 = -0.2515/r_b^3 \text{ gauss}$$

$$\bar{g}_2^0 = 0.1215/r_b^4 \text{ gauss}$$

where g 's are well-known Gauss coefficients in the spherical harmonic expansion of the magnetic field, and where r_b is the distance, measured in earth-radii, from the earth's center to the boundary of the magnetosphere at the subsolar point. Here r_b is taken to be 10 earth-radii.

A computer program has been developed to integrate the equations of motion (37) with r_0 , θ_0 , ϕ_0 , χ_0 , and η_0 as the initial conditions. For integration the Runge-Kutta method was used. In this paper, trajectories on the equatorial plane alone are discussed.

Figure 9 shows typical examples of the trajectories in the equatorial plane. The position of the point source is placed at 10 earth-radii regardless of the longitude. This assumption is made because the location of the magnetospheric boundary is not well known on the dark side of the magnetosphere, and because with a fixed r_0 we can compare trajectories starting from sources at different longitudes more directly. Here longitude, ϕ , is measured eastward from the midnight meridian; in figure 9 the midnight meridian is towards the left and the longitude increases counterclockwise.

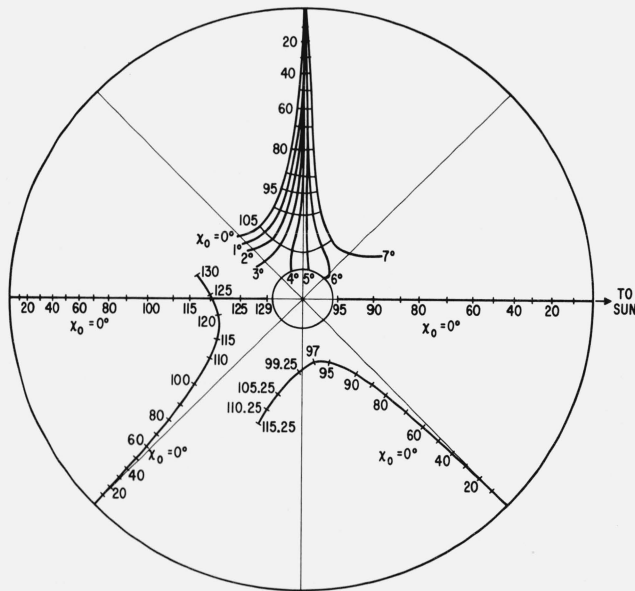


FIGURE 9. Illustrating ray trajectories in the equatorial plane in the distorted magnetosphere.

In the lower half of figure 9, trajectories starting at $\phi_0 = 0^\circ, 45^\circ, 135^\circ,$ and 180° , all with $\chi_0 = 0$ (i.e., rays directed initially towards the origin) are shown. In the upper half, trajectories with their initial position at $\phi_0 = 90^\circ$ with $\chi_0 = 0^\circ, 1^\circ, 3^\circ, 4^\circ, 5^\circ, 6^\circ,$ and 7° are drawn.

The effect of the distortion of the magnetosphere on the ray trajectories can be described by saying that hydromagnetic rays tend to be "blown" towards the direction away from the sun. This is because the magnetic field is more compressed on the sunlit side of the magnetosphere than on its dark side, thus increasing the Alfvén velocity in the region facing the sun.

However, the results presented in this section should be interpreted with caution. Although the distortion of the geomagnetic field is taken into account, possible changes in the plasma density distribution associated with the distortion are not considered here. Appreciable asymmetry may be introduced in the plasma density, but no observational data are available as yet that indicate such an effect.

The magnetic field configuration on the dark side of the magnetosphere has also not as yet been established. Since the trajectories are sensitive to large scale magnetic field patterns, the actual trajectories in the magnetosphere may be different from those shown in this paper. Our purpose is to demonstrate qualitative characteristics of ray trajectories in the magnetosphere. However, for the model used in this section the calculations are made as accurately as possible within the practical limitations.

It is observed in figure 9 that if the point source is not in the meridian containing the sun (i.e., $\phi_0 = 0^\circ$ or 180°), the ray directed initially towards the earth does not reach the earth. For the ray to reach the earth it must start with χ_0 slightly greater than 0. If χ_0 becomes too large, the ray is bent back at the region of Alfvén velocity maximum. This circumstance is shown for $\phi_0 = 90^\circ$ in the upper half of figure 9. At this ϕ_0 , rays with $\chi_0 = 3.0^\circ$ and less are "blown" towards the back of the magnetosphere. At χ_0 between 3.0° and 3.2° the ray begins to penetrate into the immediate vicinity of the earth, and this condition prevails till χ_0 reaches a value a little less than 6.5° . Beyond this latter angle the ray is again reflected away from the earth at the region of Alfvén velocity maximum.

In figure 9 the time in seconds is indicated along the trajectories. It is of interest to compare the transit time from r_0 to some altitude near the earth for the trajectory in the midnight meridian with the corresponding transit time for the trajectory in the noon meridian. In figure 9 the altitude of the point marked 95 sec in the noon meridian and the altitude of the point marked 129 sec in the midnight meridian differ only by 45 km. The mean of the two altitudes is 1,363 km above the earth's surface. Thus the difference in the transit time from 10 earth-radii to this altitude is about 34 sec. However, as has already been mentioned, caution should be exercised in applying this result to any actual events that occur in the magnetosphere.

In concluding the discussions of the ray theory the following remarks are made. The hydromagnetic approximation is based on the condition that $\omega \ll \Omega_i$. Thus for the most part of the magnetosphere this approximation is good below 10 Hz (fig. 3). There is another limitation to the ray theory, namely, that the wavelength be short compared with the dimension under consideration. We put this condition in the form $\omega \gg V/L$, where L is the typical scale length. If we take L to be the smallest value of the radius of curvature for the ray trajectories, then the minimum frequency may be set at about 1 Hz. Thus, roughly speaking, the ray theory is applicable to propagation of hydromagnetic waves of frequencies about 1 to 10 Hz.

A more extensive study of the ray trajectories in the magnetosphere and their physical implications will be reported later. For instance, the efficiency of energy transfer from solar winds to the ionosphere via hydromagnetic waves is considerably reduced by the limited accessibility of the hydromagnetic waves to the immediate vicinity of the earth.

A theoretical study of geometrical hydromagnetics based on a classical hydromagnetic fluid has been made by Bazer and Hurley [1963]; their paper includes comprehensive reference to the literature on the subject.

4. Conclusions

We reviewed the possible modes of waves in a two-component cold plasma using the Clemmow-Mullaly-Allis diagram. A systematic method of labeling the modes was explained.

The modes relevant to propagation of ULF to VLF waves in the regions of plasma parameter space representing the conditions in the magnetosphere were reviewed. For frequencies below the ion cyclotron frequency there are two modes: the *fast mode* with right-handed circular polarization for propagation along the magnetic field and with phase velocity dependent on the magnetic field for propagation across it, and the *slow mode* with left-handed circular polarization for propagation along the magnetic field. Waves in the latter mode do not propagate across the magnetic field. Above the ion cyclotron frequency, only the fast mode represents propagating wave, and above the lower hybrid resonance frequency this mode becomes the guided whistler mode.

Reversal of polarization in the electric field that could take place at a certain direction of phase propagation with reference to the direction of the magnetic field was discussed. We concluded that there is no such reversal in polarization in ULF to VLF waves in the magnetosphere.

The hydromagnetic approximation was examined and its relation to the more exact treatment was indicated.

In this paper we only discussed propagation of waves in a collisionless plasma. When the thermal motions of electrons and ions are included, the waves found in a cold plasma are modified. The modifications are

often only slight, but in a hot plasma new modes are introduced which have no counterpart in a cold plasma. There are two such modes in a relatively low-frequency range. They are ion acoustic waves and electrostatic ion cyclotron waves. These waves were not discussed in this paper; the reader is referred to discussions on these waves made, for instance, by Spitzer [1956], Bernstein [1958], and Stix [1962].

In the latter half of this paper, we changed the line of approach, and formulated a ray theory. The equations of motion of a ray were derived from a simple postulate that a ray moves with the group velocity. The action of the ray was defined with analogy to classical mechanics, and the principle of least action was proved. It was shown that the principle of least action takes the form of the principle of least time when the dispersion relation is homogeneous in the wave vector \mathbf{k} and the frequency ω .

For the case in which the wave-normal surface is spherical, a ray theory was formulated in Hamiltonian form. In the axially symmetric case the generalized momentum conjugate to the azimuthal coordinate becomes a constant of motion. Using this relation, allowed and forbidden regions were defined for a hydromagnetic ray in the magnetosphere with the magnetic field approximated by that of a dipole. It was shown that a ray originating from the magnetospheric boundary can reach the ionosphere only if the deviation of the initial direction of the ray from the meridian plane is small.

When the distortion of the geomagnetic field due to solar wind is taken into account, the ray trajectories in the magnetosphere are appreciably altered from those in a dipole field.

In spite of the limitations in its application the hydromagnetic ray theory for the magnetosphere should provide a guide towards a more complete understanding of propagation of hydromagnetic waves in the magnetosphere.

I thank W. F. Cahill for his valuable suggestions on the numerical calculations in this paper. I am indebted to W. H. Mish, Mrs. S. J. Hendricks, and Mrs. P. J. Connor for their helpful assistance in preparing the computer programs and performing the calculation.

5. References

- Alfvén, H. (1942), On the existence of electromagnetic-hydromagnetic waves, *Arkiv f. Mat.* **29B**, No. 2; Existence of electromagnetic-hydromagnetic waves, *Nature* **150**, 405-406.
- Allis, W. P. (1959), Waves in a plasma, *Sherwood Conf. Contr. Fusion, Gatlinburg, Apr. 27-28*, p. 32, TID-7582.
- Allis, W. P., S. J. Buchsbaum, and A. Bers (1963), *Waves in anisotropic plasmas* (MIT Press, Cambridge, Mass.).
- Åström, E. O. (1950), On waves in an ionized gas, *Arkiv f. Fysik* **2**, No. 42, 443-457.
- Auer, P. L., H. Hurwitz, Jr., and R. D. Miller (1958), Collective oscillations in a cold plasma, *Phys. Fluids* **1**, No. 6, 501-514.
- Bazer, J., and Hurley, J. (1963), Geometrical hydromagnetics, *J. Geophys. Res.* **68**, No. 1, 147-174.

- Beard, D. B. (1964), The solar wind geomagnetic field boundary, *Rev. Geophys.* **2**, No. 2, 335-365.
- Bernstein, I. B. (1958), Waves in a plasma in a magnetic field, *Phys. Rev.* **109**, No. 1, 10-21.
- Cahill, L. J., and P. G. Amazeen (1963), The boundary of the geomagnetic field, *J. Geophys. Res.* **68**, No. 7, 1835-1843.
- Clemmow, P. C., and R. F. Mullaly (1955), Dependence of the refractive index in magneto-ionic theory on the direction of the wave normal, *Physics of the Ionosphere: Report of Phys. Soc. Conf.* Cambridge, Sept. 1954, The Physical Society London, 340-350.
- Dessler, A. J. (1958), The propagation velocity of world-wide sudden commencements of magnetic storms, *J. Geophys. Res.* **63**, No. 2, 405-408.
- Dessler, A. J., W. E. Francis, and E. N. Parker (1960), Geomagnetic storm sudden commencement rise times, *J. Geophys. Res.* **65**, No. 9, 2715-2719.
- Francis, W. E., M. I. Green, and A. J. Dessler (1959), Hydromagnetic propagation of sudden commencements of magnetic storms, *J. Geophys. Res.* **64**, No. 10, 1643-1645.
- Goldstein, H. (1951), *Classical mechanics* (Addison-Wesley Press, Inc., Cambridge, Mass.).
- Hines, C. O. (1951), Wave packets, the Poynting vector, and energy flow: Part II-group propagation through dissipative isotropic media, *J. Geophys. Res.* **56**, No. 2, 197-206.
- Hines, C. O., (1957), Heavy-ion effects in audio-frequency radio propagation, *J. Atmospheric Terrest. Phys.* **11**, 36-42.
- Liemohn, H. B., and F. L. Scarf (1964), Whistler determination of electron energy and density distributions in the magnetosphere, *J. Geophys. Res.* **69**, No. 5, 883-904.
- Mead, G. D. (1964), Deformation of the geomagnetic field by the solar wind, *J. Geophys. Res.* **69**, No. 7, 1181-1195.
- Ness, N. F., C. S. Scarce, and J. B. Seek (1964), Initial results of the IMP-I magnetic field experiment, *J. Geophys. Res.* **69**, No. 17, 3531-3569.
- Sitenko, A. G., and K. N. Stepanov (1957), On the oscillations of an electron plasma in a magnetic field, *Soviet Phys. JETP* **4**, No. 4, 512-520.
- Spitzer, L., Jr., (1956), *Physics of fully ionized gases* (Interscience Publishers, Inc., New York, N.Y.).
- Stegelmann, E. J., and C. H. von Kenschitzki (1964), On the interpretation of the sudden commencement of geomagnetic storms, *J. Geophys. Res.* **69**, No. 1, 139-155.
- Stix, T. H. (1962), *The theory of plasma waves* (McGraw-Hill Book Co., Inc., New York, N.Y.).
- Störmer, C. (1955), *The polar aurora*, Part II, chs. I and II (Oxford Univ. Press, Oxford).
- Weinberg, S. (1962), Eikonal method in magnetohydrodynamics, *Phys. Rev.* **126**, No. 6, 1899-1909.

(Paper 69D8-545)